Cell Transplantation
2019, Vol. 28(11) 1404–1419

DOI: 10.1177/0963689718817524
journals.sagepub.com/home/cll
SAGE

Isolation and Characterization of a Human Fetal Mesenchymal Stem Cell Population: Exploring the Potential for Cell Banking in Wound Healing Therapies

Roger Esteban-Vives[1], Jenny Ziembicki[2], Myung Sun Choi[3], R. L. Thompson[4], Eva Schmelzer[1], and Jörg C. Gerlach[1]

Abstract

Various cell-based therapies are in development to address chronic and acute skin wound healing, for example for burns and trauma patients. An off-the-shelf source of allogeneic dermal cells could be beneficial for innovative therapies accelerating the healing in extensive wounds where the availability of a patient's own cells is limited. Human fetal-derived dermal fibroblasts (hFDFs) show high in vitro division rates, exhibit low immunological rejection properties, and present scarless wound healing in the fetus, and previous studies on human fetal tissue-derived cell therapies have shown promising results on tissue repair. However, little is known about cell lineage stability and cell differentiation during the cell expansion process, required for any potential therapeutic use. We describe an isolation method, characterize a population, and investigate its potential for cell banking and thus suitability as a potential product for cell grafting therapies. Our results show hFDFs and a bone marrow-derived mesenchymal stem cell (BM-MSC) line shared identification markers and in vitro multilineage differentiation potential into osteogenic, chondrogenic, and adipogenic lineages. The hFDF population exhibited similar cell characteristics as BM-MSCs while producing lower pro-inflammatory cytokine IL-6 levels and higher levels of the wound healing factor hepatocyte growth factor. We demonstrate in vitro differentiation of hFDFs, which may be a problem in maintaining long-term lineage stability, potentially limiting their use for cell banking and therapy development.

Keywords

mesenchymal stem cells, fetal-derived MSC, cell therapy, cell banking, wound healing

Introduction

In the USA, chronic wound treatments affect 6.5 million patients annually[1], and for acute wounds, 0.5 million burn cases are registered annually according to the CDC-NCHS[2]. The current standard treatment for chronic wounds combines wound debridement with negative pressure[3] followed by skin tissue grafting in severe cases. Due to an aging population and an association with vascular and metabolic diseases, the incidence of pressure ulcers, venous ulcers, and diabetic ulcers is increasing every year, with an estimated cost of 25 billion US$/year[1]. In the long term, healed wounds may form scars and contractions that, if not corrected, may lead to loss of functionality and unsatisfactory psychosocial results[4]. The dermal loss in acute wounds, such as deep partial- or full-thickness burn wounds, is associated with an economic impact of 6.2 billion US$/year[5]. Here, the current standard therapy, split-thickness skin grafts, has an impact on the burden of donor site area that is correlated to the size of the burned area. The patient's survival, recovery time, aesthetic outcome, and functionality are determined by the burn

[1] Departments of Surgery and Bioengineering, McGowan Institute for Regenerative Medicine, University of Pittsburgh, PA, USA
[2] The University of Pittsburgh Medical Center, UPMC Mercy Hospital Trauma and Burn Centers, Pittsburgh, PA, USA
[3] Oregon Health & Science University, Portland, OR, USA
[4] Allegheny Reproductive Health Center, Pittsburgh, PA, USA

Submitted: July 13, 2018. Revised: October 19, 2018. Accepted: November 14, 2018.

Corresponding Author:
Jörg C. Gerlach, Departments of Surgery and Bioengineering, McGowan Institute for Regenerative Medicine, University of Pittsburgh, 3025 East Carson Street, Suite 238, Pittsburgh, PA 15203, USA.
Email: Joerg.gerlach@cellnet.org

Fig. 1. Human fetal dermal-derived fibroblasts (hFDFs) off-the-shelf concept. Fetal dermal-derived fibroblasts are selected by mechanical disruption and cultured (A). Fibroblast-like cells are selected from other lineages using a stem cell knife (B). Cells are sorted using flow cytometry, cultured for expansion (C), and frozen (D). Conceptually, the cells will be thawed for clinical use applying a cell spray technique (E).

wound surface area and depth, time to treatment, and skin donor graft availability.

One of the major challenges in acute wound therapy on extensive and severe partial- and full-thickness burns is the limited availability of skin donor area. In chronic wound healing, however, the major challenge is the comprehension of the underlying pathology and, in some cases, the necessity of grafting after wound healing failure[6]. The various skin pathologies share the need to accelerate wound healing, a complex process that involves different tissues and cell types. In current research that focuses on understanding how dermal and epidermal cells initiate the signals that activate the quiescent stem cells to promote the wound healing process, the role of dermal cell–cell interactions is emphasized[7–10].

Different innovative applications using allogeneic cells have been developed as dermal replacements, providing a cellular component that does not require harvesting from large donor areas, reducing additional trauma and pain[11]. The clinical use of such allogeneic cell-based therapies has increased during the last decade, and includes products such as Dermagraft®[12], Apligraft®[13], and Stratagraft®[14]. These bioengineered allogeneic skin constructs have been tested in clinical trials to address chronic wounds and burn wound healing[15–17]. Although there are potential benefits of using bioengineered skin substitutes, no overall satisfying therapy is yet established[18].

An autologous cell source for such therapy development using fat tissue-derived mesenchymal cells[19] is under investigation, and some clinical applications have already been tested[20]. Another promising technology is the use of multipotent stem cells including bone marrow-derived mesenchymal stem cells (BM-MSCs) as allogeneic cell therapy to accelerate wound healing. Using MSCs as an off-the-freezer cell-based technology has advantages including a reported low immunogenic response and their described tissue regeneration capacities by the release of cytokines and growth factors that are thought to reduce inflammation and promote collagen deposition[21]. Several groups have studied the role of BM-MSCs in dermal wound healing processes, emphasizing their role in inflammatory processes, cell recruitment, and skin homeostasis maintenance[8,9,22–24], and clinical tests have been initiated[25].

Mesenchymal fetal skin-derived fibroblast mesenchymal lines have shown multipotent MSC properties[26], a potential for scar-free tissue repair[27], low immunological rejection properties[28,29], and high division rates[30], and thus may have a potential for clinical grafting. Due to limited availability, it requires an in vitro expansion step to guarantee enough cell lines for cell banking. Expanded human fetal tissue-derived dermal fibroblast (hFDF) lines have been previously tested as a temporary skin substitute in burn wound healing[31,32]. These characteristics would make such allogeneic of-the-freezer products interesting for potential applications in wound healing[32] on deep-extensive wound injuries (Fig. 1). However, cell isolation and establishment of human fetal mesenchymal hFDF lines, their characterization, and possible differentiation during cell culture over time is not well studied.

In this study, we established isolation and culture of an hFDF cell line. We provide information on cell characterization and cell line stability during in vitro expansion, with an outlook toward cell banking.

Materials and Methods

Skin Tissue

De-identified 9–11-week fetal skin tissue specimens (n=20) were obtained under IRB exemption approval (PR007060159, University of Pittsburgh) from the Allegheny Reproductive Health Center, Pittsburgh, Pennsylvania. Prior to cell isolation, the specimens were exposed to a storage time of 2–3 h at 4°C in phosphate buffered saline (PBS) (Invitrogen, Carlsbad, CA, USA) containing 100 U/ml penicillin, 100 µg/ml streptomycin (Invitrogen), and 2.50 µg/ml Amphotericin B (Invitrogen).

Hematoxylin and Eosin Histology

Pieces of the skin biopsies were embedded in polyvinyl-based medium Tissue-Tek (Sakura Finetek, Torrance, CA, USA) and prepared for tissue sectioning by immersing them in liquid nitrogen and pre-cooled 2-methyl butane (Sigma-Aldrich, St. Louis, MO, USA). After cutting and dehydration in gradual series of ethanol, 3 μm sections were stained with hematoxylin and eosin (Bio-Optica, Milan, Italy). Light microscopy was performed using a Nikon Eclipse 50i microscope with Nikon DS Fi1 camera and software for image acquisition (Nikon, Tokyo, Japan).

Fetal Dermal Fibroblast Isolation

Dermal tissue sections were processed following a modification of a previously described method[33]. The fetal dermal tissue sections were disaggregated using scalpel and forceps as described and cultured in a 60 mm Petri dish. The tissue was then cultured using MSCGM LONZA medium (LONZA, Basel, Switzerland) to let cells outgrow from the tissue, for further cell expansion. Pre-cultured fibroblast-like cells were then maintained in a Petri dish, and all other cell lineages were morphologically identified and removed by using a stem cell knife (Vitrolife AB, Göteborg, Sweden) and a Nikon SMZ1000 stereomicroscope (Nikon).

Fetal Dermal Fibroblast Culture

After the primary pre-culture was stabilized, 3×10^5 fibroblasts were expanded in 150 cm^2 flasks at a density of 2,000 cells/cm^2. Standard cultures were maintained in a CO_2 incubator (Heraeus BB 6060, Kendro, CORNING, Corning, NY, USA) at 37°C in a humidified atmosphere with 5% CO_2. After cell isolation and during passages, cells were cultured in MSCGM medium (LONZA). The medium was changed every 3 days. As 80% confluence was reached, cells were detached using 0.05% trypsin 0.2% EDTA (Gibco, Thermofisher, Waltham, MA, USA), and 3×10^5 cells were passaged to a new flask. Cell suspensions were counted using a Neubauer hemocytometer (Merck, Darmstadt, Germany). Culture quality control, microbiology testing, and morphology examination was done with phase-contrast microscopy using an Axiovert 25 microscope (Zeiss, Göttingen, Germany). The cell expansion rate (k) was calculated using the cell doubling time formula $x_f=x_0e^{(t*k)}$, where x_0 is the initial number of seeded keratinocytes, x_f is the final number of the harvested population, and t is the time that the hFDFs were in culture.

Mesenchymal Stem Cell Culture

For this study, 7×10^5 frozen MSCs (LONZA) were thawed and seeded according to the manufacturer's instructions. MSC cultures were maintained and expanded in vitro in MSCGM medium (LONZA) in the same manner as hFDF cells for comparable results. The medium was changed every 3 days. Cells were passaged at 80% cell confluence.

Adipogenic, Chondrogenic, and Osteogenic Differentiation Assay

hFDFs were cultured in parallel with BM-MSCs with three technical repeats for each lineage to determine osteogenic, adipogenic, and chondrogenic differentiation (LONZA). For osteogenic differentiation, cells received the induction of B-glycerophosphate and dexamethasone, and calcium deposition was detected by Alizarin Red (IHC World, Woodstock, MD, USA). Adipogenic differentiation was triggered with dexamethasone in combination with IBMX (3-isobutyl-1-methylxanthine), and oil droplets were stained with Oil Red O (Scytek, Logan, UT, USA). Chondrogenic differentiation was induced with TGF-β3, and the cells were centrifuged and cultured as a pellet. After 2–3 weeks, pellets were stained with Alcian blue for proteoglycans (Scytek).

Flow Cytometry and Cell Sorting

Cultured cells were disaggregated with 0.05/0.02% trypsin-EDTA (Gibco) and washed twice in cold PBS and centrifuged at low speed (300 *g*) for 5 min. The cells were re-suspended for 15 min with 100 μl blocking buffer/10^6 cells per tube and kept in ice. The blocking buffer contained 1% of human FcR block (Miltenyi Biotec, Bergisch Gladbach, Germany), 5% goat serum (Sigma), and 94% PBS (Gibco). Cells were stained for 30 min at 4°C with primary antibodies using stem cell markers CD105-FITC, CD90-PerCPCy5.5, CD73-APC, CD34-APC, CD45-FITC, CD14-PerCPCy5.5, CD79α-APC, and HLA-DR-FITC in a concentration determined by the vendor (BD, Becton Dickinson, Franklin Lakes, NJ, USA). After three washes with BD Perm/Wash™ buffer (BD), the cells were fixed with 4% paraformaldehyde. For MACS cell sorting, cells were pre-treated in the same manner and incubated for 30 min at 4°C with the Miltenyi specific antibodies CD105, CD34, CD45 (Miltenyi Biotec) using different combinations. Cells were sorted using the MS Miltenyi columns (Miltenyi Biotec) and washed three times with MACS buffer. Depending on the sorting strategy, the sorted cells were retained in the column or the supernatant. Cells were centrifuged 5 min at 300 *g* and re-suspended in MSCGM medium (LONZA). hFDF populations (n=5) were sorted using fluorescence-activated cell sorting (FACS) (BD FACS Aria II, Becton Dickinson) marker strategy using CD105-V450, CD90-PerCPCy5.5, CD73-PE, CD34-AF700, CD45-APCH7, CD14-FITC, CD79α-APC, and HLA-DR-FITC. Compensation beads (BD) were stained with the same markers as positive controls. Isotype controls were used as negative controls at the same concentration as the primary antibodies. Cells were sorted at 800–3,200 cells/s and maintained at 4°C in Buffered Solution MACS (Miltenyi Biotec) at Buffer pH 7.25, and afterward cultured in MSCGM medium (LONZA). After cell sorting, sorted populations (n=3) were cultured for six passages and analyzed to measure the MSC-like population maintenance. We have

assumed between 0.1 to 5% error defining the gating strategy to calculate the percentage of MSC population.

Gene Expression Analysis

Gene expression analyses were done directly from harvested cells, after isolation or after in vitro culture. The mRNA was extracted from 3×10^5 cultured hFDFs (n=6) and BM-MSCs (n=3) at different passages using the RNAeasy Purification Kit (Qiagen, Venlo, Netherlands). The mRNA was reverse transcribed into cDNA using a Transcription Assay (Applied Biosystems, Life Technologies, Grand Island, NY, USA). Reverse transcriptase reaction was performed at 25°C (10 min), 37°C (120 min), and 85°C (5 min). The cDNA from different donors and passages were analyzed using a Real-Time Polymerase Chain Reaction (Applied Biosystems) with TaqMan probe and primer mixes for the genes CD105, CD90, CD73, CD34, CD45, CD14, CD79α, and HLA-DR. We also tested the genes HGF, Il-6, ELN, Col1A, Col2A, Ki67 comparing cultured BM-MSCs (Fig. 2C, Fig. 3D, E, K) or hFDFs 2D-cultured cells versus 3D culture (Fig. 5A, B). PCR temperature and time conditions were: 50°C (2 min) 1 cycle, 95°C (10 min) 1 cycle, and 95°C (15 s) plus 60°C (1 min), for 40 cycles. The gene expression was shown as relative quantification using the mean comparative method Delta-Delta CT ($\Delta\Delta C_T$). The levels of mRNA for every sample were normalized to βACT housekeeping gene expression.

Immunofluorescence Staining Assays

Cells cultured in a four-well chamber slide (Thermo Scientific, Rochester, NY, USA) were rinsed with PBS and fixed with methanol/acetone. Sections were permeabilized using PBS with 1% Triton 100 (PBS, Sigma-Aldrich) and blocked with PBS with 1% Triton 100, FcR (Miltenyi Biotec, Auburn, CA), goat serum (Sigma-Aldrich), for 1 h at room temperature. Primary antibodies used were CD105, CD90, and CD73 (Novus Biologicals, Littleton, CO, USA). After overnight incubation in a humid chamber at 4°C with the primary antibody, secondary staining was done with a secondary AF488 antibody (Invitrogen) for 1 h at room temperature. Samples were washed three times with PBS-triton and were mounted using Aqua Poly/Mount (Polysciences, Warrington, PA, USA). Cells were studied using a Nikon Eclipse 50i microscope with a Nikon DS Fi1 camera and software for image acquisition (Nikon) and Olympus Fluoview 1000 confocal microscopy (Olympus, Center Valley, PA, USA) at CBI (University of Pittsburgh Medical School, Pittsburgh, PA, USA).

Interleukin 6 (IL-6) and Hepatocyte Growth Factor (HGF) Enzyme-Linked Immunosorbent Assay (ELISA)

IL-6 and HGF ELISAs were performed using sorted cell populations (n=3) with three technical repetitions. 10^5 cells were cultured during three passages in a 9.6 cm^2 well and compared with bone marrow mesenchymal stromal cells (LONZA) at passage 2. Cells were cultured using 2 ml MSCGM medium (LONZA), and the medium was collected when cells reached 80% of confluence. New culture medium was added and harvested after 48 h of culture. IL-6 and HGF were quantified with an ELISA kit (Peprotech, Rocky Hill, NJ, USA), using a Synergy H1 plate reader (Biotek, Winooski, VT, USA). Data were normalized to the number of cells.

Contraction Assay

A cell contraction assay (Cell Biolabs, San Diego, CA, USA) was performed with three different cell lineages donors D31, D34, and D36 of fetal dermal derived cells and one lineage of MSCs (LONZA), all of which were sorted and cultured for two passages. A total of 1×10^5 cells from each donor was mixed with collagen I matrix and added to 6 wells. After 48 hours in culture, cells mixed with collagen matrix were physically detached from the edge of the well and the discs were analyzed for matrix contraction. Three wells were used as negative contraction controls by adding 2,3 butanedione monoxime (BDM) to inhibit the myosin II contraction. The collagen lattice contraction was measured as a change in mm after 20 h.

Scratch Assay

Three frozen sorted ($CD105^+$, $CD73^+$, $CD90^+$, $CD34^-$, $CD45^-$) fetal-derived fibroblast lines (hFDF D31, D34, and D36) and one MSC lineage were seeded for expansion during 6 days; 10,000 cells of every lineage were passaged in a 4-well chamber (ThermoFisher, Waltham, MA, USA). The cells were settled for 2 days, and the scratch was performed using a 10 μm pipette tip, and the cell migration was analyzed at time 0, 24, and 48 h. Pictures were acquired using Nikon Eclipse 50i microscope with a Nikon DS Fi1 camera (Nikon). The total cultured area was 1.7 cm^2 but the "wound closure" measurement was limited to the optical field (approximately 1 mm^2) and represented by a percentage. The wound healing measurement was determined by delimiting the empty spots with Photoshop CS3 (Adobe Systems Incorporated, San Jose, CA, USA) and measured the area with Image J software (NIH, Bethesda, MD, USA)[34].

Statistical Analyses

The statistical test used in the analysis of changes in MSC markers gene expression of cultured hFDFs was a two-way ANOVA with a Sidak's multiple comparison tests. The sources of variation analyzed were five genes (CD105, CD90, CD73, CD34, CD45) and two passages groups (passages #2–3 and #4–7). We investigated the division rate differences of sorted and non-sorted fetal dermal-derived fibroblasts from n=20 independent skin donations comparing follow-up cultures from passages 1–3, 4–6 with passages 1–3 of MSCs (n=3). One-way ANOVA with Dunnett's multiple tests was performed for all analysis combining data from different passages and comparing the cell sorting method.

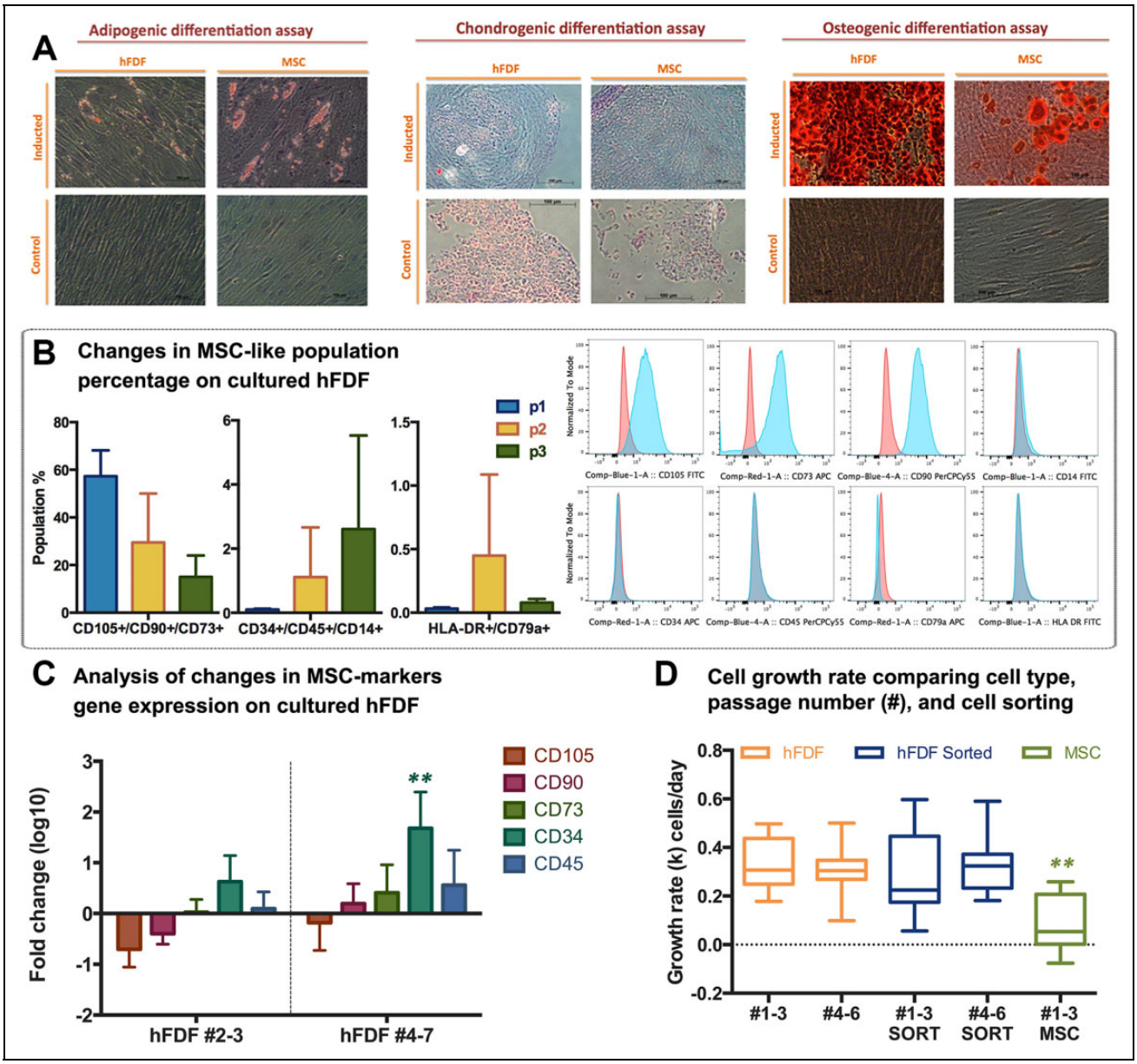

Fig. 2. Detection of mesenchymal stem cell (MSC) population in human fetal dermal-derived fibroblasts (hFDFs). (A) Adipogenic, chondrogenic and osteogenic differentiation of hFDF cells compared with bone marrow (BM)-MSCs as a positive control. Adipogenic differentiation was induced by IBMX (3-isobutyl-1-methylxanthine), and staining was done with Oil Red O for fatty acids. Chondrogenic differentiation was induced by TGF-β3, and cells were stained with Alcian blue for proteoglycans. Osteogenic differentiation was induced by B-Glycerophosphate, and cells were stained with Alizarin S red for calcium deposition. (B) Flow cytometry chart showing percentages of mesenchymal stem cell antigen markers of passages #1–3 of cultured 9–11-week-old fetal dermal fibroblasts (n=6). Isotypes (red) and human fetal-derived fibroblast signal (blue). Maximum gate error of 5%. (C) Gene expression analysis for markers CD105, CD90, CD73, CD34, CD45 of different hFDF lineages (n=6), comparing passages 2–3 (n=6) with hFDF passages 4–7 (n=4), normalized to bone marrow mesenchymal stromal cells (n=3). (D) Cell growth rate analysis, comparing the doubling time (k) among hFDF donors (n=20) of passages 1–3 and 4–6, with/without sorting and MSC (n=3). ** (p<0.01).

The statistical analysis for the contraction assay was an ANOVA with a Sidak's multiple analysis tests. The test compared independent samples (n=3) from different lineages of hFDFs (n=3) and MSCs (n=1). All tests were performed using the statistics software Prism vs6 (GraphPad Software, La Jolla, CA, USA).

Results

hFDF Population Showed in vitro Multipotency

The fetal dermal-derived fibroblasts cell populations (hFDFs) were induced to show in vitro multipotency in comparison to human MSCs. hFDF lineages were initially

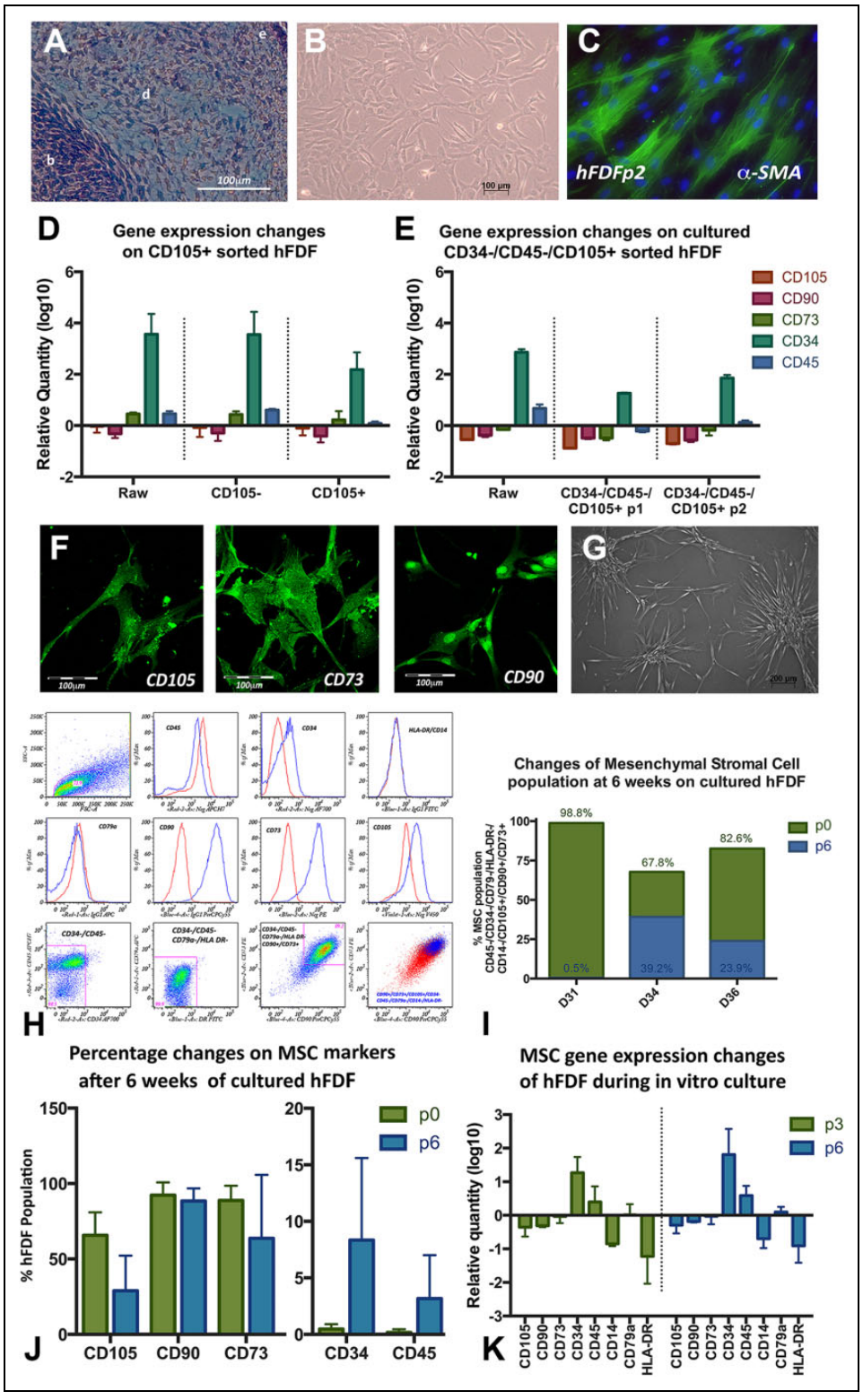

Fig. 3. Sorted hFDF populations showing differentiation after 6 in vitro passages. (A) Skin biopsy section of 10 weeks gestational age, showing human fetal dermal fibroblasts before isolation. Other cell lineages are visible such as bone (b), dermis (d), and epidermis (e). (B) outgrowth of hFDF cells after isolation. (C) Differentiated hFDF cells at passage 2 expressing α-SMA. (D) Gene expression analysis of MACS CD105$^{+/-}$ sorted hFDF cells (n=2) compared with the raw population. (E) Gene expression analysis of passages 1 and 2 of MACS CD34^{-}/CD45^{-}/CD105^{+} sorted hFDF cells (n=2) compared with the raw population. (F) Immunofluorescence staining of MSC-like population surface antigen markers CD105, CD90, CD73 present in hFDF populations before sorting. (G) Sorted hFDF population in vitro during expansion. (H) Flow Cytometry sorting strategy showing mesenchymal stem cell antigen marker isotypes (red) and human fetal-derived fibroblast signals (blue). Max gate error=5%. (I) hFDF population percentage showing MSC antigen markers CD105^{+}/CD90^{+}/CD73^{+}/CD34^{-}/CD45^{-}/CD14^{-}/CD79α^{-}/HLA-DR^{-} after sorting (p0) and after 6 weeks (p6) in culture. (J) Flow cytometry analysis is showing changes in percentages of hFDF cells presenting the individual MSC markers CD105, CD90, CD73, CD34 and, CD45 after sorting compared with 6 weeks in culture. (K) Gene expression analysis of MSC markers of hFDF populations between passage 3 (n=3) and 6 (n=3). (D, E, and J) Gene expression results were normalized to mesenchymal stem cell populations, using beta-actin as a housekeeping gene.

expanded and, after induction, and proteoglycan staining showed positive staining for all three tests, revealing osteogenic, adipogenic and chondrogenic differentiation, respectively (Fig. 2A).

hFDFs Exhibited MSC Phenotype

Isolated hFDF populations from six independent donors were cultured for three passages and characterized by flow cytometry using MSC markers proposed by the ISCT[35]. Expanded cells on passage 1 showed a population positive for MSC markers with a mean of 57% for the $CD105^+$/$CD90^+$/$CD73^+$, 0.1% for the $CD34^+$/$CD45^+$/$CD14^+$, and 0.03% for $CD79a^+$/HLA-DR^+ (Fig. 2B). hFDF cells on passage 3 decreased to 15% of the $CD105^+$/$CD90^+$/$CD73^+$ population, increased to 2.6% $CD34^+$/$CD45^+$/$CD14^+$, and maintained a percentage less than 0.1% for $CD79a^+$/HLA-DR^+. During expansion, hFDF cells showed a progressive decrease in gene expression for BM-MSC markers CD105 and CD90 and an increase for CD34 and CD45, suggesting the cells were starting to differentiate compared to BM-MSCs (Fig. 2C). Further gene expression analyses on passages 4 to 7 confirmed the decrease of CD105, and the increase of CD34 and CD45 compared with BM-MSCs.

hFDF Suitability for Cell Banking

hFDF cells from 20 donors were independently cultured, comparing the cell expansion rates between unsorted hFDFs, MSC markers-sorted hFDF cell lineages, and BM-MSC lineages. We did not find significant statistical differences in growth rates (k=0.30–0.33 cells/day) among hFDF cell lineages and passages, making them suitable for cell banking (Fig. 2D). However, division rates of BM-MSCs (k=0.08 cells/day) were significantly lower ($p<0.05$) than those of hFDF cell lineages.

Differentiation Analysis of Sorted Human Fetal Dermal-Derived Fibroblasts

We sorted the hFDF population to obtain a highly enriched MSC-like population cell source minimizing initial cell population mixture using a combination of antibody and column method (Miltenyi) (Fig. 3D). We sorted the initial population by enriching in $CD105^+$ cells, but the gene expression analysis still showed low CD105 expression, with an increase of CD34 expression (Fig. 3E). Next, we repeated the cell sorting including staining with CD34 and CD45 to enrich the final cell population with cells that were CD34– and CD45–, and $CD105^+$. Gene expression analysis for $CD105^+$/$CD34^-$/$CD45^-$sorted cells, cultured for 2 weeks, showed a reduction of CD45 and CD34 expression compared with the raw population (Fig. 3E). However, this cell sorting was still insufficient to sort and maintain the $CD105^+$ population, and cells still differentiated to $CD34^+CD45^+$. We also observed a gene expression reduction of the $CD90^+$, $CD73^+$ cell population. Therefore, we decided to sort the initial population with FACS using a complete MSC markers panel.

A large MSC marker panel for flow cytometry cell-sorting step was included to ascertain that all cells in culture contained the MSC markers CD105, CD90, and CD73 (Fig. 3F, H) and did not contain CD45, CD34, CD79α, or HLA-DR (Fig. 3H). The hFDF lineages presented different initial MSC population percentages before sorting, with 67.6% for Donor 31, 61.2% for Donor 34, and 48.4% for Donor 36. After the sorting process, isolated cells (Fig. 3G) had a purity of 98.8% for donor 31, 67.8% for donor 34, and 82.6% for donor 36 (Fig. 3I). Initially, sorted cells had the appearance of spheroids (Fig. 3G), and during the expansion of cell numbers showed fibroblast-like appearance. Sorted hFDF lineages were cultured for 6 weeks, and the population percentage was expressing the MSC markers analyzed with flow cytometry. After six passages, cultured hFDF Donor 31 showed 0.53% of MSC markers, donor 34 had 39.2%, and donor 36 had 23.9% (Fig. 3I).

Stemness Marker Expression over Passaging

Flow cytometry analysis on individual markers of hFDFs after 6 weeks of expansion showed a negative 2-fold change of CD105, CD90, and CD73 markers, and a 2- and 3-fold increase in CD34 and CD45, respectively (Fig. 3J). Gene expression showed a decrease in CD105, CD90, and CD90, and markers CD34 and CD45 increased on passages 3 and 6 compared with BM-MSCs passage 2 control (Fig. 3K). This gene expression analysis revealed that sorted cells differentiated as previously observed (Fig. 2C), and gene expression demonstrated similar trends as observed in flow cytometry (Fig. 3J).

hFDFs Secrete Paracrine Effectors Involved in Wound Healing

MSCs play a role in skin homeostasis and regeneration after an injury by migrating into the wound[36], and by releasing paracrine effectors to recruit different cell lineages[9] that make them valuable for a wide variety of wound healing therapies. Despite the fact that hFDFs and MSCs share stem cell markers, we analyzed their capability of releasing the paracrine effectors HGF and IL-6, which are involved in wound healing. Sorted hFDF cells and MSCs were cultured in triplicate to passage 3 and 2, respectively, to measure the secreted paracrine effectors interleukin 6 (IL-6) and HGF that are involved in wound healing (Fig. 4A). hFDF released 100 pg/ml ($\pm$53.48) IL-6, a significantly lower amount of IL-6 compared with 752.2 pg/ml ($\pm$85.86) released by MSCs. On the other hand, hFDF cells secreted 335.6 pg/ml HGF ($\pm$138.6) compared with 35.8 pg/ml HGF ($\pm$5.7) released by MSCs.

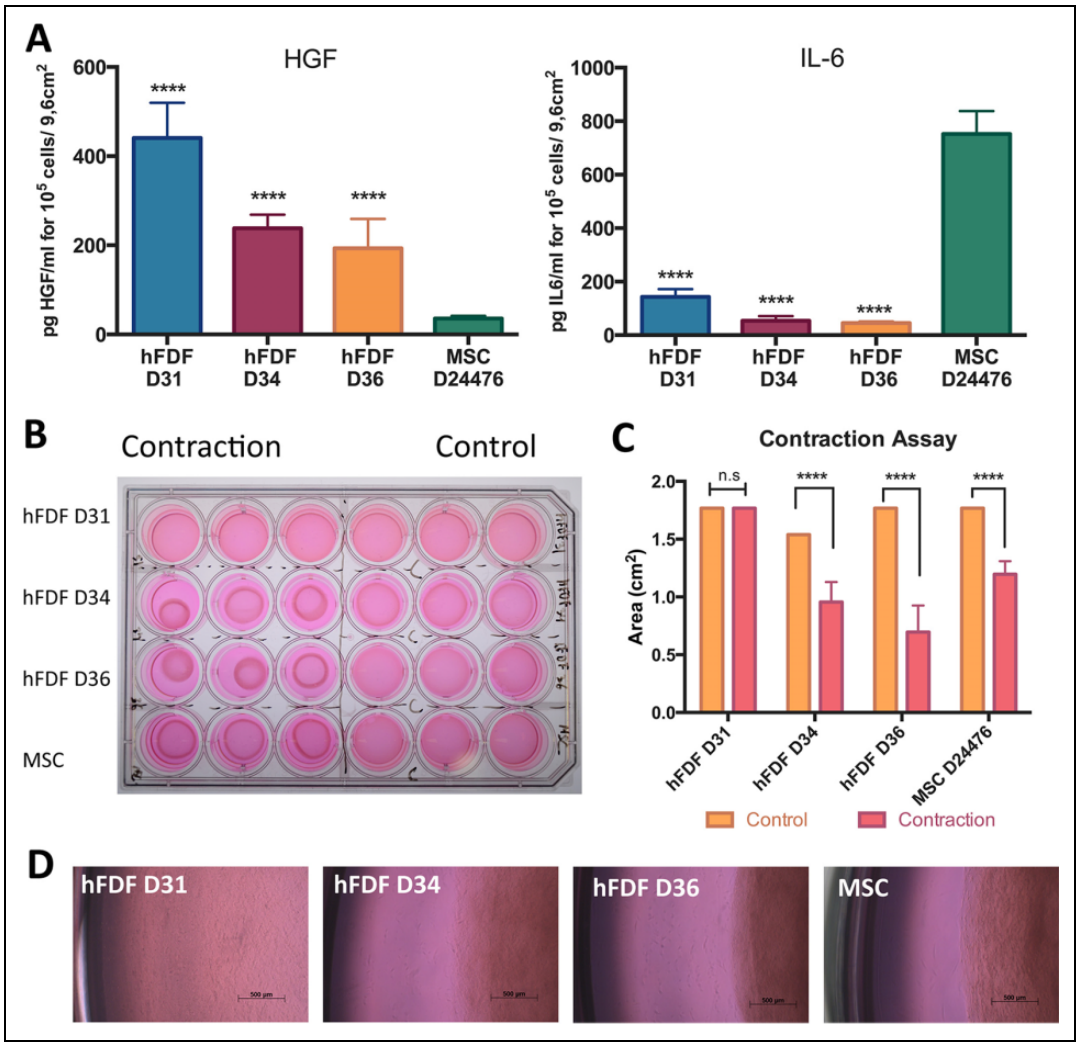

Fig. 4. Cytokine secretion and contraction assay comparing hFDFs and MSCs. (A) Secretion of interleukin 6 (IL-6) and hepatocyte growth factor (HGF) of fetal dermal-derived fibroblasts at passage 3 compared with mesenchymal stromal cells at passage 2. The HGF and IL-6 concentration were normalized to the cell number in the culture at 48 h (pg/ml per well). (B) 10^5 cells of passage 2 fetal dermal-derived cells or mesenchymal stem cells were mixed with collagen I matrix. After 48 h in culture, cells mixed with collagen matrix were physically detached from the edge of the well and the discs were analyzed for matrix contraction. Results show the contraction after 20 h. 2,3 butanedione monoxime (BDM) was used to inhibit contraction (control). (C) Contraction is given as area; the same samples, cultured with (BDM) or without (control) inhibitor for contraction. (D) Detail of the cells and collagen matrix disc edge.

Fetal Dermal-Derived Cells Combined with Collagen I Biomatrix Change their Gene Expression Pattern

hFDFs embedded within a collagen type I biomatrix were tested looking for potential contraction capability (Fig. 4B–D). The collagen lattice contraction assay revealed that hFDFs D31 did not show contraction in any of the three repeats, while D34, D36, and hMSCs showed a statistically significant degree of contraction ($p<0.0001$) compared with the negative control group with inhibited contraction with BDM (Fig. 4C). The ≈0.5 cm^3 collagen discs for donors 34, 36, and MSCs were shrunk by the cell contraction effect and reduced in their area by 38%, 61%, and 32%, respectively, compared with negative controls. We also detected changes in the gene expression when comparing all the cell lines growth in conventional culture to those embedded in a collagen matrix (Fig. 5A). We observed an increase of expression in genes like elastin (ELN), collagen type 1 alpha-A1 (Col 1A), collagen type 1 alpha-A2 (Col 2A), and HGF on hFDF and MSC cell lines when cultured on a 3D collagen matrix compared with the same cell lines cultured in 2D. On the other hand, we observed a reduction of Ki67 gene expression in all cell lineages. IL-6 gene expression was reduced in all cell lines except for D36. When the gene expression was compared through all the cell lines expanded in conventional culture (Fig. 5B), IL-6 expression was similar in Donor 34 and MSCs, but reduced in Donor 31 and particularly low in Donor 36. Donor 36 showed significantly reduced expression in genes ELN and Col 1 2A, compared with the other

cell groups. Donor 31 and 34 showed a similar gene expression pattern on ELN, Col 1 A1, and Col 1 A2, and all donors showed a 6–20 fold increase in HGF expression compared with MSC.

Differentiated Fetal Dermal-Derived Cells Migrate Faster

Wound healing capability was analyzed using the scratch test where cells migrated from the wound edge after a scratch on the surface (Fig. 6). The initial damaged area represented 41–64% of the visual field area (approximately 1 mm^2). Cells from the edge of the "wound" filled the gap by division and/or migration. The hFDF D31 and 36 filled around 99.5% of the gap in 24 h and hFDF D34 needed some more hours, but in 48 h the three cell lineages already filled the similar area. However, MSCs were only able to cover up to 25% of the wounded area in 48 h. MSCs had a lower cell division rate and thus did not cover the entire surface before the scratch test started.

Discussion

The Potential use of hFDFs as a Therapeutic Cell Source

Human fetal dermal-derived fibroblasts could be of interest in regenerative medicine, for their potential use in wound healing therapies due to their skin remodeling ability, their cell banking feasibility[30], and their multipotent cell characteristics[26]. The hFDF population we described shares a comparable cell lineage origin with the analyzed MSCs that we used as a control, along with the same characterization markers[37], multipotency[26,38], and partially low immunological response[28,39,40], making hFDFs interesting for allogeneic transplantation. We confirmed that the isolated hFDF population expresses cell markers comparable with the investigated MSCs (Fig. 2B) and showed multipotency in vitro by differentiating under induced stimuli into osteogenic, chondrogenic, and adipogenic cell lineages (Fig. 2A).

Mammalian fetal tissue showed high plasticity recovering from wound injuries, especially at early developmental stages[27], with scarless fetal tissue regeneration in humans being observed before 24 weeks of gestational age[41]. In wound healing therapies hFDFs have already been clinically tested in pediatric burn patients and showed reduced healing time while maintaining resulting functionality[31,42]. The same study also demonstrated that allogeneic cells used in the healing process were no longer present in the body after 6 months[31]. However, little is known about the potential differentiation of hFDFs after cell isolation during the cell banking expansion process.

Cell Expansion and Banking Ability

Our findings also revealed that hFDF cell populations have a high division rate (Fig. 2D) compared with adult-derived MSC cell lines, due to their cell age as has been described in the literature[43]. hFDF cells also presented fast wound closures in scratch tests, showing higher migration rates (Fig. 6). High division rates make an hFDF ideal in cell banking as a cell source for an off-the-shelf skin replacement (Table 1). Previous studies in fetal dermal cell banking comparing different seeding cell densities between 3,000 and 6,000 cells/cm^2 showed that higher cell densities have higher cell culture cycles and still had enough cells for banking[30]. Other studies using 20–22-week fetal dermal cells showed that passaging at higher cell densities maintained stable MSC populations during longer cycles[38]. However, the methodology used in such studies only focused on independent single marker analysis along the passages instead of a complete MSC markers panel suggesting low differentiation. We revealed how hFDF populations differentiate during cell expansion showing significant differences when cell populations are analyzed by flow cytometry using a multiple marker panel (Fig. 3I) or analyzing one-by-one single markers (Fig. 3J).

Difficulties in Maintaining a Stable Undifferentiated Cell Population

The cell isolation method used for the dermal tissue does not allow obtaining a pure source of fetal dermal fibroblasts[33]. The cell outgrowth method (Fig. 3A, B) expanded a different variety of dermal cell lineages, where the detection of α-SMC (Fig. 3C) suggests that the initial cell population might contain a subset of smooth muscle cells or pericytes[44]. During the cell isolation process, different cell lineages might have been expanded and still included in the final population (Fig. 3A, B). Between 40% and 50% (Fig. 2B) of the initially isolated cells did not show MSC markers, and those cells could be responsible for differentiation by competition during the expansion process. Also, gene expression analysis during the initial expansion revealed changes in the hFDF populations, where cells started to differentiate into cells expressing $CD105^-/CD34^+/CD45^+$ (Fig. 2C).

Our results sorting $CD105^+/CD34^-/CD45^-$ cells using magnetic bead separation showed an ineffective sorting method, revealing a loss of CD105 marker expression along with increases in $CD34^+CD45^+$ cell marker expression (Fig. 3D, E). These results suggested that cultured hFDFs started differentiation. To exclude a methodological issue or artifact-caused differentiation, we sorted the initially expanded cell population using flow cytometry with the MSC markers[35] panel $CD105^+/CD90^+/CD73^+/CD34^-/CD45^-/CD14^-/CD79a^-$/HLA-$DR^-$.

The cell expansion step was followed by cell characterization after 3 and 6 weeks, analyzing changes in the population using the MSC markers panel. After 6 weeks of cell expansion, hFDF lineages had lost the $CD105^+$ population, while increasing the percentage of $CD34^+$, $CD45^+$, and maintaining stable $CD90^+$, and $CD73^+$ markers (Fig. 3J). These results were consistent with gene expression analysis changes (Fig. 3K).

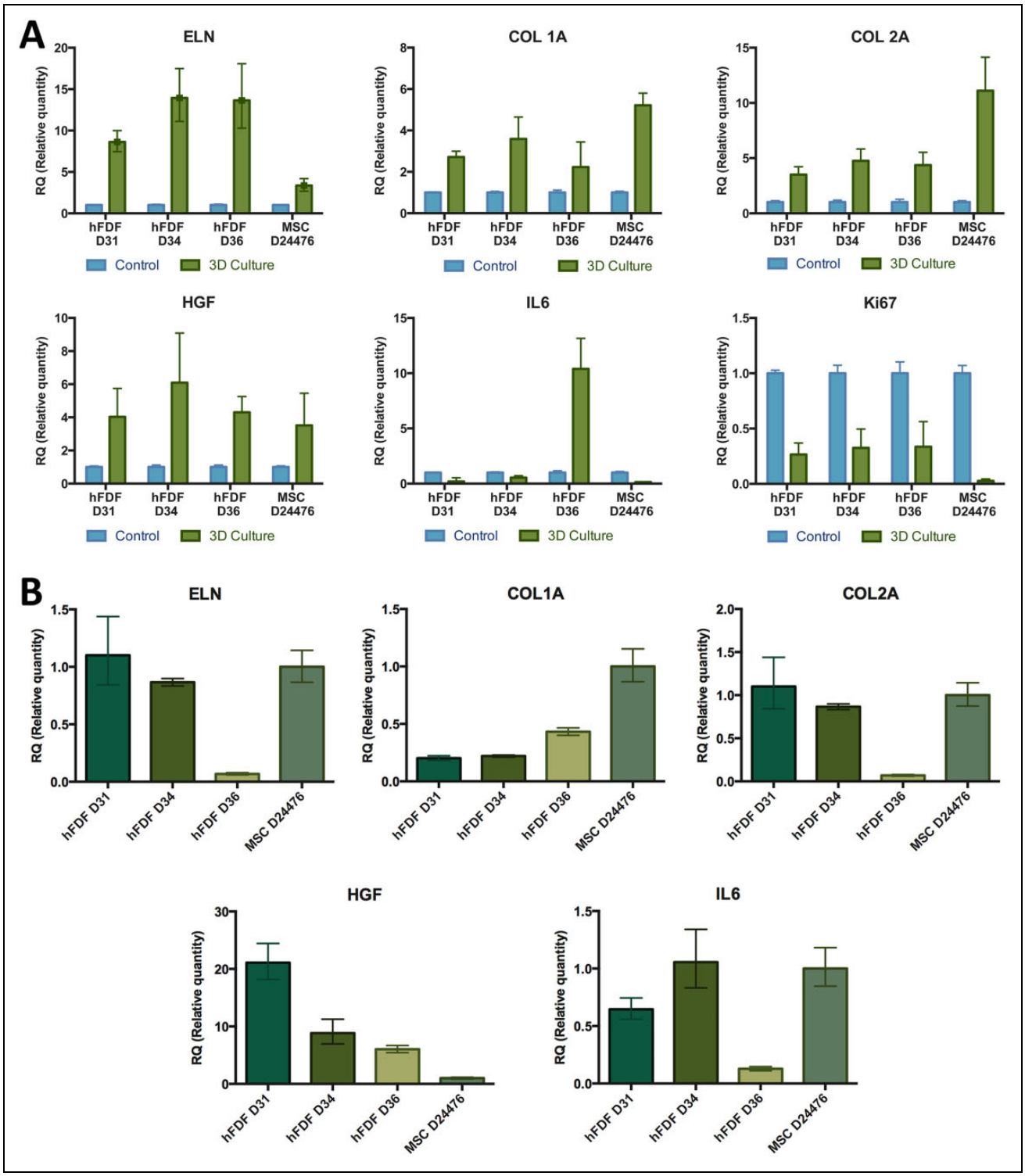

Fig. 5. Gene expression of cultured cells in collagen I matrix. (A) Gene expression analyses of hFDF and MSC donors embedded in collagen I matrix (3D culture) compared with their correspondent 2D cultured homologs (controls). (B) Gene expression analysis of different hFDF cell lineages cultured in 2D compared with MSCs as a control. Data are given as mean from three technical repeats $\pm$ standard error. Results are presented as $\Delta\Delta C_T$ mean, normalized to beta-actin housekeeping gene expression. ELN: Elastin; Col 1A: Collagen 1A; Col2B: Collagen 2B; HGF: Hepatocyte growth factor; IL-6: Interleukine-6; ki67: proliferation protein.

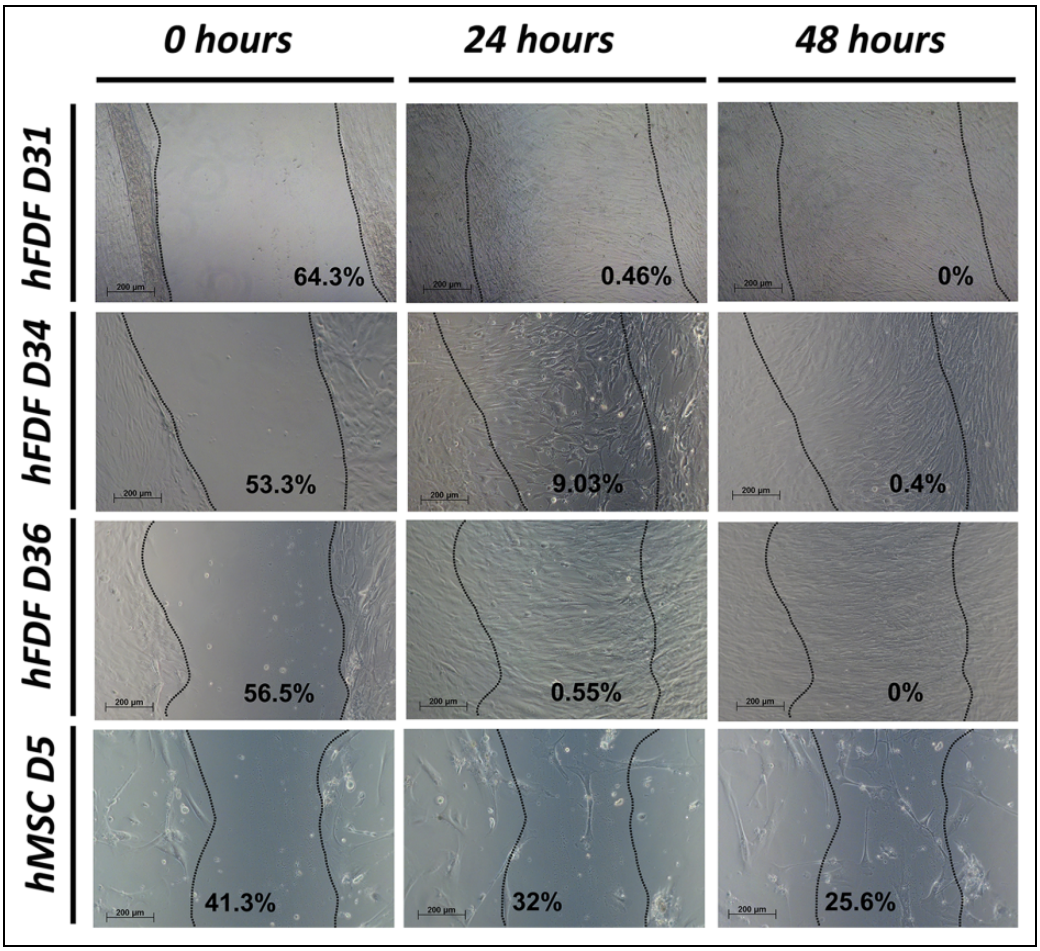

Fig. 6. Scratch assay to test wound healing capabilities measuring the cell migration after 24 and 48 h. The open wound area is represented by the percentage of scratched surface without cell coverage.

Table 1. Cell division rate (k) comparing passages (#) between sorted (SORT), non-sorted hFDFs and MSCs. #

Lineage	Fetal-derived dermal fibroblasts (hFDFs)				Mesenchymal stem cells (MSCs)
Passage	#1–3 SORT	#4–6 SORT	#1–3	#4–6	#1–3
Growth rate (k)	0.3006	0.3231	0.3302	0.3101	0.07786
std. deviation	0.1630	0.1048	0.1	0.099	0.1190

Anderson et al. described that differences in CD105 expression could be a consequence of the culture process, and specifically due to cell confluence[45]. They found that a decrease in $CD105^+$ population could be a selection and expansion of a different subset of the population, rather than differentiation, and the $CD105^-$ subpopulation would still have a high ability to differentiate into adipocytes and osteocytes[45]. Fathke et al. showed that BM-MSCs used in wound healing in a rat model differentiate into endothelial $CD34^+$ and fibrocyte-type $CD45^+$ cell lineages[21]. Kaiser et al. sorted bone marrow-derived cells based on the expression of $CD34^+$ and $CD45^+$ for subsequent analysis of the MSC content. They did not find MSCs in the $CD45^+/CD34^+$ seeded subpopulation and concluded that BM-MSCs expressing $CD34^+/CD45^+$ are not able to attach[46]. However, we observed stable hFDF $CD34^+/CD45^+$ subpopulations that attached and expanded in vitro.

The Potential Advantage of Differentiated hFDFs During Wound Healing

Studies with embryonic stem cells describe low percentages of $CD34^+$ cell lineages that were stable in culture and were able to become MSC progenitor cells[47]. Postnatal ESC-

derived $CD34^+$ cells showed an adherent fibroblast-like phenotype, and multipotent characteristics and functionality compared with BM-MSCs. Other studies disclosed that $CD34^+$ cell lineages are a type of peripheral blood osteoblast precursor involved in bone repair[48,49].

Huang et al. found that foreskin-derived fibroblasts presented some similarities with BM-MSCs, being able to differentiate into adipocytes and osteocytes, but that they were not able to express $CD105^{+}$[50]. Another hypothesis about the low levels of CD105 would be linked to the effects that high levels of HGF have on TGF-b1. Endoglin is part of the TGF complex that modulates, via TGF-b1-induction, the synthesis of ECM-like molecules. Endoglin plays a role maintaining the balance of collagen I deposition on fibroblasts by blocking TGF-β1[51]. One possible explanation of the low $CD105^+$ population is that TGF-β1 could be inhibited by HGF, negatively selecting the $CD105^+$ population by repressing its expression. That would explain why D31 has a lower MSC population percentage compared with D34, D36, and MSC D24476 (Fig. 3I, Fig. 4A, Fig. 5B). Whiteley et al. showed that a cultured subpopulation of umbilical cord-derived $CD34^+$ MSCs showed the high potential of regeneration in of ischemic injury after transplantation, by recruiting endogenous cells via paracrine signaling and directly, through *in situ* engraftment, differentiating into capillaries, smooth muscle, and minor striated regeneration[52].

It is also remarkable that hFDFs and MSCs showed a very low HLA-DR expression, suggesting a very low or no immune response (Fig. 2B and Fig. 3K). Some studies suggest that MSC have an inhibitory effect on T-cell proliferation[53]. They are thought to show a low immunologic response by triggering tryptophan catabolism, which in turn inhibits T-cell proliferation[28], although other studies showed that MSC lineages are not intrinsically immune privileged[54]. However, assays in burned patients showed that hFDF cells embedded in constructs remain in the wound for a limited period until they are replaced by autologous cells[55].

Fetal Dermal Cells, Paracrine Effectors, and Wound Regeneration Properties

hFDF cell lineages showed wound healing capability in the scratch tests (Fig. 6), where in 24 h the cells migrated from the wound edge into the empty area covering 90–99% of the "wound." Even though MSC lineage was seeded with the same initial cell number, MSCs did not have the same initial cell coverage due to the slow cell division ability. Independently of the cell division rate, both hFDFs and MSCs showed migration capability to cover the wound gap.

Fetal-derived cells showed higher division rates than adult cells, but when we normalize the cell number, hFDF populations release in the medium higher concentrations of HGF and lower concentrations of IL-6 compared with MSC controls. Our results have also shown that hFDFs from various donors produce different concentrations of HGF, which inversely correlates with the percentage of the MSC population (Fig. 3I, Fig. 4A). In our results an increase of HGF production correlated with an increase in dermal differentiation. At the same time, HGF concentrations produced by hFDF cells and HGF gene expression are inversely correlated with collagen 1 A1 expression in hFDFs and MSCs (Fig. 5B). In the literature, it has been shown that concentrations of HGF show a negative correlation with collagen 1 A1 and αSMA expression, suggesting an anti-fibrotic effect during wound healing[56].

HGF plays an important role in the wound healing process by stimulating epithelial cells[23] and enhancing wound closure[57]. Other studies showed that HGF suppresses the TGF-β1 production of BM-MSCs by temporarily suppressing T-lymphocyte proliferation[53]. Highly proliferative fibroblasts can contribute to excessive collagen I deposition. However, HGF has the effect of inhibiting the MSC proliferation, stimulating their migration[58]. HGF also modulates tissue fibrosis during the progression of chronic diseases by reducing the collagen deposition of fibroblasts and inhibiting the plasminogen activator inhibitor, an ECM-degrading enzyme inhibitor[59].

The pro-inflammatory cytokine IL-6 is secreted by adult fibroblasts in large quantities, stimulating the recruitment of monocytes by chemotaxis and macrophages activation[9]. The presence of IL-6, secreted in burn wound blisters[60], may be involved in stimulating keratinocyte migration[61] and keratinocyte proliferation[62]. Duncan and Berman showed that adult dermal fibroblasts could produce constitutive levels of IL-6 (0.5–0.8 ng/ml) that could play a role in wound repair during dermal fibrotic remodeling[63]. Gallucci et al. showed that an IL-6 concentration of 100 pg/ml exhibited the best keratinocyte migration response, while IL-6 knockout mice presented a significant wound healing delay[64,65]. On the other hand, IL-6 above 500 pg/ml showed migration reduction triggered by feedback inhibition[61]. Although IL-6 plays an important role during the acute phase response to an injury, an excessive concentration of circulating cytokines is associated with morbidity and mortality in burns and acute trauma injuries[66,67]. A low concentration of IL-6 in fetal wound healing is associated with a low inflammatory response, which in turn creates a permissive environment for scarless skin regeneration[68]. Our results showed that sorted hFDF cells produced low concentrations of the pro-inflammatory cytokine IL-6 compared with MSCs. The constitutive production of IL-6 in hFDF cells combined with bioengineered skin tissue may be even lower (Fig. 5A), which would be beneficial by avoiding the pro-inflammatory local response and its long-term pathologic effect, especially during the remodeling phase.

hFDFs in Collagen I Embedded Constructs

The results of the collagen contraction assay showed a donor-dependent high variability response shrinking the lattice (Fig. 4B, C). In addition, changes in the gene expression

of hFDFs and MSCs comparing traditional 2D culture with collagen I matrix embedded cells reveal substantial changes that may affect the skin functionality (Fig. 5A, B). Comparisons among the hFDF and MSC donors on HGF gene expression (Fig. 5B) matched with the quantified cytokine production in 2D culture (Fig. 4A). However, IL-6 gene expression and cytokine quantification showed some differences between the protein quantification and the gene expression. One possible explanation would be post-transcriptional regulation, or significant differences could be attributed to the limitation of the gene expression as a one-time point analysis.

These results are important because they consider that wound healing and tissue regeneration bear different meanings, implying that an excessive increase of collagen deposition combined with wound contraction may end up in scar formation. The division is inhibited in all cell lineages once cells are embedded in a collagen I matrix as Ki67 marker decreases.

Conclusion

We previously introduced employing clinically adult epidermal stem cell preparations for autologous cell spray-grafting in severe partial-thickness II° burns. There, a cell isolation technique for basal epidermal progenitors was introduced[33,69]. Including primary passage zero dermal cells into such innovative therapies could be of interest[70,71], and combinations with cultured and banked hFDFs could be of special value for extensive critical full-thickness burns[72] (Fig. 1).

The expansion of fetal dermal skin-derived fibroblasts was tested, showing inherent characteristics that would be beneficial for wound healing therapies. However, we were unable to maintain lineage stability after 6 weeks of culture under our tested conditions. We demonstrate that the cell lineage fate—besides the initial tissue source and after cell sorting with specific markers—may determine the suitability for cell banking and thus the feasibility for being used as potential therapeutic. Despite the hFDF potential for wound healing, the cell source origin may face some objection to public acceptance.

Further studies involving clonogenic expansion are required to ensure cell lineage stability, maintaining of cell fate, and controlling differentiation processes. Of interest would be studies on hFDF functionality when embedded in 3D matrix structures that more resemble skin conditions in vivo.

Author contributions

RE and JG wrote the manuscript. RE and JG designed and coordinated the experimental design. RE performed cell isolations, in vitro culture work, and RE and MS did the molecular assays. AC, JZ, and all other authors evaluated data, revised the manuscript, and provided discussions.

Acknowledgments

We wish to thank all staff of the Allegheny Reproductive Health Center for continuous help and support. In memory of Morris Edward Turner, MD, who gently contributed to this research with dedication and passion. We thank Matt Young for assistance in cell isolation, culture, and characterization. We also thank StemCell Systems, Berlin, Germany for providing technology.

Ethical Approval

This study was conducted under IRB exemption approval (PR007060159, University of Pittsburgh, Pittsburgh, PA, USA).

Statement of Human and Animal Rights

No studies were performed on humans or animals.

Statement of Informed Consent

No human subjects were treated in this work, no informed consent was applicable.

Declaration of Conflicting Interests

The author(s) declared the following potential conflicts of interest with respect to the research, authorship, and/or publication of this article: JG has a potential conflict of interest through the support of the work by StemCell Systems, Berlin, Germany and RenovaCare, New York in which he has a financial interest. Roger Esteban-Vives is a consultant to RenovaCare Inc.

Funding

The author(s) disclosed receipt of the following financial support for the research, authorship, and/or publication of this article: This research was partly funded through the AFIRM-I consortium (Project UPitt 4.2.2, 2009-2013) by the US Department of Defense.

References

1. Sen CK, Gordillo GM, Roy S, Kirsner R, Lambert L, Hunt TK, Gottrup F, Gurtner GC, Longaker MT. Human skin wounds: a major and snowballing threat to public health and the economy. Wound Repair and Regen. 2009;17(6):763–771.
2. National hospital ambulatory medical care survey: 2011 emergency department summary. 2011. [accessed July 7]. http://www.cdc.gov/nchs/ahcd/web_tables.htm#2011.
3. Argenta LC, Morykwas MJ. Vacuum-assisted closure: a new method for wound control and treatment: clinical experience. Ann Plast Surg. 1997;38(6):563–577.
4. Balakrishnan C, Hashim M, Gao D. The effect of partial-thickness facial burns on social functioning. J Burn Care Rehabil. 1999;20(3):224–225.
5. Corso P, Finkelstein E, Miller T, Fiebelkorn I, Zaloshnja E. Incidence and lifetime costs of injuries in the united states. Inj Prev. 2006;12(4):212–218.
6. Snyder RJ. Treatment of nonhealing ulcers with allografts. Clin Dermatol. 2005;23(4):388–395.
7. Martin P. Wound healing – aiming for perfect skin regeneration. Science. 1997;276(5309):75–81.
8. Aoki S, Toda S, Ando T, Sugihara H. Bone marrow stromal cells, preadipocytes, and dermal fibroblasts promote epidermal

regeneration in their distinctive fashions. Mol Biol Cell. 2004; 15(10):4647–4657.
9. Liwen Chen EET, Philip Y. G. Wu, Yaojiong Wu. Paracrine factors of mesenchymal stem cells recruit macrophages and endothelial lineage cells and enhance wound healing. PLoS One. 2008;3(4):e1886.
10. SA McClain MS, Jones E, Nandi A, Gailit JO, Tonnesen MG, Newman D, Clark RA. Mesenchymal cell activation is the rate-limiting step of granulation tissue induction. Am J Pathol. 1996;149(4):1257–1270.
11. Auger F, Rouabhia M, Goulet F, Berthod F, Moulin V, Germain L. Tissue-engineered human skin substitutes developed from collagen-populated hydrated gels: clinical and fundamental applications. Med Biol Eng Comput. 1998;36(6):801–812.
12. Gentzkow GD, Iwasaki SD, Hershon KS, Mengel M, Prendergast JJ, Ricotta JJ, Steed DP, Lipkin S. Use of dermagraft, a cultured human dermis, to treat diabetic foot ulcers. Diabetes care. 1996;19(4):350–354.
13. Eaglstein WH, Falanga V. Tissue engineering and the development of Apligraf®, a human skin equivalent. Clin Ther. 1997;19(5):894–905.
14. Ji L, Allen-Hoffmann BL, Pablo JJD, Palecek SP. Generation and differentiation of human embryonic stem cell-derived keratinocyte precursors. Tissue Eng. 2006;12(4):665–679.
15. Veves A, Falanga V, Armstrong DG, Sabolinski ML. Graftskin, a human skin equivalent, is effective in the management of noninfected neuropathic diabetic foot ulcers a prospective randomized multicenter clinical trial. Diabetes Care. 2001; 24(2):290–295.
16. Harding K, Morris H, Patel G. Healing chronic wounds. BMJ. 2002;324(7330):160–163.
17. Schurr MJ, Foster KN, Centanni JM, Comer AR, Wicks A, Gibson AL, Thomas-Virnig CL, Schlosser SJ, Faucher LD, Lokuta MA. Phase I/II clinical evaluation of Stratagraft: a consistent, pathogen-free human skin substitute. J Trauma. 2009;66(3):866–873.
18. Shores JT, Gabriel A, Gupta S. Skin substitutes and alternatives: a review. Adv Skin Wound Care. 2007;20(9):493–508.
19. Pittenger MF, Mackay AM, Beck SC, Jaiswal RK, Douglas R, Mosca JD, Moorman MA, Simonetti DW, Craig S, Marshak DR. Multilineage potential of adult human mesenchymal stem cells. Science. 1999;284(5411):143–147.
20. García-Olmo D, García-Arranz M, Herreros D, Pascual I, Peiro C, Rodríguez-Montes JA. A phase I clinical trial of the treatment of crohn's fistula by adipose mesenchymal stem cell transplantation. Dis Colon Rectum. 2005;48(7):1416–1423.
21. Fathke C, Wilson L, Hutter J, Kapoor V, Smith A, Hocking A, Isik F. Contribution of bone marrow-derived cells to skin: collagen deposition and wound repair. Stem Cells. 2004; 22(5):812–822.
22. Koskela A, Engstrom K, Hakelius M, Nowinski D, Ivarsson M. Regulation of fibroblast gene expression by keratinocytes in organotypic skin culture provides possible mechanisms for the antifibrotic effect of reepithelialization. Wound Repair Regen. 2010;18(5):452–459.
23. Shamis Y, Hewitt KJ, Carlson MW, Margvelashvilli M, Dong S, Kuo CK, Daheron L, Egles C, Garlick JA. Fibroblasts derived from human embryonic stem cells direct development and repair of 3D human skin equivalents. Stem Cell Res Ther. 2011;2(1):10.
24. Wu Y, Chen L, Scott PG, Tredget EE. Mesenchymal stem cells enhance wound healing through differentiation and angiogenesis. Stem Cells. 2007;25(10):2648–2659.
25. Falanga V, Iwamoto S, Chartier M, Yufit T, Butmarc J, Kouttab N, Shrayer D, Carson P. Autologous bone marrow-derived cultured mesenchymal stem cells delivered in a fibrin spray accelerate healing in murine and human cutaneous wounds. Tissue Eng. 2007;13(6):1299–1312.
26. Covas DT, Panepucci RA, Fontes AM, Silva WA Jr, Orellana MD, Freitas MC, Neder L, Santos AR, Peres LC, Jamur MC, Zago MA. Multipotent mesenchymal stromal cells obtained from diverse human tissues share functional properties and gene-expression profile with CD146+ perivascular cells and fibroblasts. Exp Hematol. 2008;36(5):642–654.
27. Longaker MT, Stern M, Lorenz P, Whitby DJ, Dodson TB, Harrison MR, Adzick NS, Kaban LB. A model for fetal cleft lip repair in lambs. Plast Reconstr Surg. 1992;90(5):750–756.
28. Munn DH, Zhou M, Attwood JT, Bondarev I, Conway SJ, Marshall B, Brown C, Mellor AL. Prevention of allogeneic fetal rejection by tryptophan catabolism. Science. 1998; 281(5380):1191–1193.
29. Zuliani T, Saiagh S, Knol A-C, Esbelin J, Dreno B. Fetal fibroblasts and keratinocytes with immunosuppressive properties for allogeneic cell-based wound therapy. PLoS One. 2013; 8(7):e70408.
30. Quintin A, Hirt-Burri N, Scaletta C, Schizas C, Pioletti DP, Applegate LA. Consistency and safety of cell banks for research and clinical use: preliminary analysis of fetal skin banks. Cell Transplant. 2007;16(7):675–684.
31. Hohlfeld J, de Buys Roessingh A, Hirt-Burri N, Chaubert P, Gerber S, Scaletta C, Hohlfeld P, Applegate LA. Tissue engineered fetal skin constructs for paediatric burns. Lancet. 2005; 366(9488):840–842.
32. De Buys R, Anthony S, Hohlfeld J, Scaletta C, Hirt-Burri N, Gerber S, Hohlfeld P, Gebbers J-O, Applegate LA. Development, characterization, and use of a fetal skin cell bank for tissue engineering in wound healing. Cell Transplant. 2006; 15(8–9):823–834.
33. Johnen C, Chinnici C, Triolo F, Plettig J, Bräutigam K, Amico G, Young M, Over P, Esteban-Vives R, Schmelzer E, Conaldi PG, et al. Phenotypical characterization of 6–21-week gestational age human dermis and epidermal cell isolation methods for in vitro studies on epidermal progenitors. Burns. 2013; 39(2):300–310.
34. Rasband WS. Imagej. Bethesda, MA: US National Institutes of Health; 1997–2015.
35. Dominici M, Le Blanc K, Mueller I, Slaper-Cortenbach I, Marini F, Krause D, Deans R, Keating A, Prockop D, Horwitz E. Minimal criteria for defining multipotent mesenchymal stromal cells. The International Society for Cellular Therapy position statement. Cytotherapy. 2006;8(4):315–317.

36. Badiavas EV, Abedi M, Butmarc J, Falanga V, Quesenberry P. Participation of bone marrow derived cells in cutaneous wound healing. J Cell Physiol. 2003;196(2):245–250.
37. Akershoek J, Vlig M, Talhout W, Boekema B, Richters C, Beelen R, Brouwer K, Middelkoop E, Ulrich M. Cell therapy for full-thickness wounds: are fetal dermal cells a potential source? Cell Tissue Res. 2015;364(1):83–94.
38. Chinnici CM, Amico G, Monti M, Motta S, Casalone R, Petri SL, Spada M, Gridelli B, Conaldi PG. Isolation and characterization of multipotent cells from human fetal dermis. Cell Transplant. 2014;23(10):1169–1185.
39. Sundin M, Barrett AJ, Ringden O, Uzunel M, Lonnies H, Dackland AL, Christensson B, Blanc KL. HSCT recipients have specific tolerance to MSC but not to the MSC donor. J Immunother. 2009;32(7):755–764.
40. Bartholomew A, Sturgeon C, Siatskas M, Ferrer K, McIntosh K, Patil S, Hardy W, Devine S, Ucker D, Deans R. Mesenchymal stem cells suppress lymphocyte proliferation in vitro and prolong skin graft survival in vivo. Exp Hematol. 2002;30(1): 42–48.
41. Larson BJ, Longaker MT, Lorenz HP. Scarless fetal wound healing: a basic science review. Plast Reconstr Surg. 2010; 126(4):1172–1180.
42. Hirt-Burri N, Ramelet AA, Raffoul W, de Buys Roessingh A, Scaletta C, Pioletti D, Applegate LA. Biologicals and fetal cell therapy for wound and scar management. ISRN Dermatol. 2011;2011:549870.
43. Allsopp RC, Chang E, Kashefi-Aazam M, Rogaev EI, Piatyszek MA, Shay JW, Harley CB. Telomere shortening is associated with cell division in vitro and in vivo. Exp Cell Res. 1995; 220(1):194–200.
44. Paquet-Fifield S, Schlüter H, Li A, Aitken T, Gangatirkar P, Blashki D, Koelmeyer R, Pouliot N, Palatsides M, Ellis S, Brouard N, Zannettino A, Saunders N, Thompson N, Li J, Kaur P. A role for pericytes as microenvironmental regulators of human skin tissue regeneration. J Clin Invest. 2009;119(9): 2795–2806.
45. Anderson P, Carrillo-Gálvez AB, García-Pérez A, Cobo M, Martín F. CD105 (endoglin)-negative murine mesenchymal stromal cells define a new multipotent subpopulation with distinct differentiation and immunomodulatory capacities. PLoS One. 2013;8(10):e76979.
46. Kaiser S, Hackanson B, Follo M, Mehlhorn A, Geiger K, Ihorst G, Kapp U. BM cells giving rise to MSC in culture have a heterogeneous CD34 and CD45 phenotype. Cytotherapy. 2007;9(5):439–450.
47. Kopher RA, Penchev VR, Islam MS, Hill KL, Khosla S, Kaufman DS. Human embryonic stem cell-derived CD34+ cells function as MSC progenitor cells. Bone. 2010;47(4): 718–728.
48. Matsumoto T, Kawamoto A, Kuroda R, Ishikawa M, Mifune Y, Iwasaki H, Miwa M, Horii M, Hayashi S, Oyamada A. Therapeutic potential of vasculogenesis and osteogenesis promoted by peripheral blood CD34-positive cells for functional bone healing. Am J Pathol. 2006;169(4):1440–1457.
49. Chen JL, Hunt P, McElvain M, Black T, Kaufman S, Choi EH. Osteoblast precursor cells are found in CD34+ cells from human bone marrow. Stem Cells. 1997;15(5):368–377.
50. Huang HI, Chen SK, Ling QD, Chien CC, Liu HT, Chan SH. Multilineage differentiation potential of fibroblast-like stromal cells derived from human skin. Tissue Eng Part A. 2010;16(5): 1491–1501.
51. Rodríguez-Barbero A, Obreo J, Álvarez-Muñoz P, Pandiella A, Bernabéu C, Novoa J. Endoglin modulation of TGF-ß1-induced collagen synthesis is dependent on ERK1/2 MAPK activation. Cell Physiol Biochem. 2006;18(1–3):135–142.
52. Whiteley J, Bielecki R, Li M, Chua S, Ward MR, Yamanaka N, Stewart DJ, Casper RF, Rogers IM. An expanded population of CD34+ cells from frozen banked umbilical cord blood demonstrate tissue repair mechanisms of mesenchymal stromal cells and circulating angiogenic cells in an ischemic hind limb model. Stem Cell Rev. 2014;10(3):338–350.
53. Di Nicola M, Carlo-Stella C, Magni M, Milanesi M, Longoni PD, Matteucci P, Grisanti S, Gianni AM. Human bone marrow stromal cells suppress t-lymphocyte proliferation induced by cellular or nonspecific mitogenic stimuli. Blood. 2002;99(10): 3838–3843.
54. Nauta AJ, Westerhuis G, Kruisselbrink AB, Lurvink EGA, Willemze R, Fibbe WE. Donor-derived mesenchymal stem cells are immunogenic in an allogeneic host and stimulate donor graft rejection in a nonmyeloablative setting. Blood. 2006;108(6):2114–2120.
55. Applegate LA, Scaletta C, Hirt-Burri N, Raffoul W, Pioletti D. Whole-cell bioprocessing of human fetal cells for tissue engineering of skin. Skin Pharmacol Physiol. 2009;22(2):63–73.
56. Schievenbusch S, Strack I, Scheffler M, Wennhold K, Maurer J, Nischt R, Dienes HP, Odenthal M. Profiling of anti-fibrotic signaling by hepatocyte growth factor in renal fibroblasts. Biochem Biophys Res Commun. 2009;385(1):55–61.
57. Chandrasekher G, Kakazu AH, Bazan HE. HGF- and KGF-induced activation of pi-3k/p70 s6 kinase pathway in corneal epithelial cells: its relevance in wound healing. Experimental eye research. 2001;73(2):191–202.
58. Neuss S, Becher E, Wöltje M, Tietze L, Jahnen−Dechent W. Functional expression of HGF and HGF receptor/c−met in adult human mesenchymal stem cells suggests a role in cell mobilization, tissue repair, and wound healing. Stem Cells. 2004;22(3):405–414.
59. Mou S, Wang Q, Shi B, Gu L, Ni Z. Hepatocyte growth factor suppresses transforming growth factor-beta-1 and type III collagen in human primary renal fibroblasts. Kaohsiung J Med Sci. 2009;25(11):577–587.
60. Ono I, Gunji H, Zhang JZ, Maruyama K, Kaneko F. A study of cytokines in burn blister fluid related to wound healing. Burns. 1995;21(5):352–355.
61. Gallucci RM, Sloan DK, Heck JM, Murray AR, O'Dell SJ. Interleukin 6 indirectly induces keratinocyte migration. J Invest Dermatol. 2004;122(3):764–772.
62. Nelson AM, Katseff AS, Ratliff TS, Garza LA. Interleukin 6 and stat3 regulate p63 isoform expression in keratinocytes during regeneration. Exp Dermatol. 2016;25(2):155–157.

63. Duncan MR, Berman B. Stimulation of collagen and glycosaminoglycan production in cultured human adult dermal fibroblasts by recombinant human interleukin 6. J Invest Dermatol. 1991;97(4):686–692.
64. Gallucci RM, Simeonova PP, Matheson JM, Kommineni C, Guriel JL, Sugawara T, Luster MI. Impaired cutaneous wound healing in interleukin-6–deficient and immunosuppressed mice. FASEB J. 2000;14(15):2525–2531.
65. Lin Z-Q, Kondo T, Ishida Y, Takayasu T, Mukaida N. Essential involvement of IL-6 in the skin wound-healing process as evidenced by delayed wound healing in IL-6-deficient mice. J Leukoc Biol. 2003;73(6):713–721.
66. Biffl WL, Moore EE, Moore FA, Barnett CC Jr., Carl VS, Peterson VN. Interleukin-6 delays neutrophil apoptosis. Arch Surg. 1996;131(1):24–29; discussion 29–30.
67. Meduri GU, Headley S, Kohler G, Stentz F, Tolley E, Umberger R, Leeper K. Persistent elevation of inflammatory cytokines predicts a poor outcome in ards. Plasma IL-1 beta and IL-6 levels are consistent and efficient predictors of outcome over time. Chest. 1995;107(4): 1062–1073.
68. Liechty KW, Adzick NS, Crombleholme TM. Diminished interleukin 6 (IL-6) production during scarless human fetal wound repair. Cytokine. 2000;12(6):671–676.
69. Johnen C, Steffen I, Beichelt D, Brautigam K, Witascheck T, Toman N, Moser V, Ottomann C, Hartmann B, Gerlach JC. Culture of subconfluent human fibroblasts and keratinocytes using biodegradable transfer membranes. Burns. 2008;34(5): 655–663.
70. Gerlach JC, Johnen C, McCoy E, Brautigam K, Plettig J, Corcos A. Autologous skin cell spray-transplantation for a deep dermal burn patient in an ambulant treatment room setting. Burns. 2011;37(4):e19–e23.
71. Gerlach JC, Johnen C, Ottoman C, Brautigam K, Plettig J, Belfekroun C, Munch S, Hartmann B. Method for autologous single skin cell isolation for regenerative cell spray transplantation with non-cultured cells. Int J Artif Organs. 2011;34(3): 271–279.
72. Hartmann B, Ekkernkamp A, Johnen C, Gerlach JC, Belfekroun C, Köntscher MV. Sprayed cultured epithelial autografts for deep dermal burns of the face and neck. Ann Plast Surg. 2007;58(1):70–73.